



# Estimating the physical properties of slags

by K.C. Mills\*, L. Yuan\*, and R.T. Jones†

## Synopsis

The objective of this work was to provide process engineers with values of the physical properties of various slag systems involved in high-temperature processes. Software that calculates the thermo-physical properties of slags from chemical composition is available on the [www.pyrometallurgy.co.za](http://www.pyrometallurgy.co.za) website. This paper outlines the principles underlying the various models available in the program. The software calculates the following properties of crystalline, glassy, and liquid slags (where appropriate) as a function of temperature: heat capacity, enthalpy, density, viscosity, thermal conductivity, electrical conductivity, and surface tension. We hope, in the future, to update the program to (i) add new models as they become available, (ii) remove any 'bugs' discovered in existing programs, and (iii) provide guidance on the limitations of individual programs.

## Keywords

pyrometallurgy, molten, slag, physical properties, heat capacity, enthalpy, density, viscosity, thermal conductivity, electrical conductivity, surface tension.

## Introduction

Slags play an important part in many processes in metal production and refining, coal gasification, continuous casting, etc. The properties of these slags have a significant effect on the performance of the process, e.g. the selection of viscosity and solidification temperature are key to minimizing defects in the continuous casting of steel<sup>1</sup>, and the electrical conductivity of the slag determines the power supply requirements of many electric smelting processes<sup>2</sup>. The physical properties of these slags are needed to solve process problems and to improve product quality. However, in recent years there has been an exponential increase in the use of mathematical models to solve process and quality problems, and these models require reliable input data for the physical properties of the slags used in the process. As there are a large number of processes, a wide range of slag compositions used in any one process, and a large number of properties involved, there is a need for a vast amount of property data. The measurement of thermo-physical

properties of molten slags is both difficult and expensive. Consequently, there has been a drive to develop empirical rules and models to estimate the various properties of slags from their chemical compositions, as this information is available on a routine basis. Furthermore, the properties of glasses and enamels are also related to those of slags, and so the models developed can, in some cases, be applied to these materials too.

A significant number of models have been reported to estimate the thermo-physical properties of slags. For some properties (e.g. viscosity) there are a large number of reported models available, whereas, in other cases, there are few reported models (e.g. electrical and thermal conductivities) and these are frequently available only for either simple slag systems (e.g. ternaries) or for a limited compositional range.

Silicates are the basis of most metallurgical slags, and their physical properties are very dependent on the silicate structure developed in the molten slag<sup>3</sup>. The dependence of property on structure is in the hierarchy, viscosity ( $\eta$ ) > electrical conductivity ( $\kappa$ ) and thermal conductivity ( $k$ ) > thermal expansion coefficient ( $\alpha$ ) > density ( $\rho$ ) > surface tension ( $\gamma$ ) >  $C_p$  and enthalpy. In fact, some workers have proposed that the viscosity is a convenient form to represent slag structure<sup>4,5</sup>. In recent years, the capabilities of commercial thermodynamic software packages have expanded from the estimation of thermodynamic properties to the estimation of parameters to represent the slag structure and which lead to the calculation of slag densities and viscosities<sup>6-10</sup>. The reliability of the property values estimated by the various

\* Department of Materials, Imperial College, London.

† Pyrometallurgy Division, Mintek, Randburg, South Africa.

© The Southern African Institute of Mining and Metallurgy, 2011. SA ISSN 0038-223X/3.00 + 0.00. This paper was first presented at the Southern African Pyrometallurgy Conference, 6-9 March 2011, Misty Hills, Muldersdrift.

## Estimating the physical properties of slags

thermodynamic packages will be evaluated in the future. Most process engineers do not have either the time or the specific expertise required to implement the reported models. Consequently, we have developed here a simple program that will enable engineers to estimate thermo-physical properties from the chemical composition of the slag in mass per cent.

### Objectives of this work

The objectives of this work are:

- To develop a program to calculate various physical properties of slags from their chemical compositions and to make this openly available by placing it on the [www.pyrometallurgy.co.za](http://www.pyrometallurgy.co.za) website
- To write a set of notes to accompany the program to aid its use, point out the limitations of predictions of individual models, range of applicability, etc., and provide guidance on which model to use for the slag system in question
- To identify any 'bugs' within the program and correct them continually
- To add new models as they become available.

### Effect of structure and other factors on properties

A full list of the symbols and abbreviations used is given at the end of this paper.

### Structure of silicate and alumino-silicate slags

Slags are formed of ions, and slag reactions are electro-chemical in nature, involving the exchange of ions. Slags contain two forms of bonds: (i) covalent Si-O bonds that form into chains, rings etc., and (ii) ionic bonds involving cations such as Na<sup>+</sup> or Ca<sup>2+</sup> that break the silicate chains, etc., to form Na<sup>+</sup>-O<sup>-</sup> bonds<sup>11</sup>. The silicate structural unit (SiO<sub>4</sub><sup>4-</sup>) consists of one Si<sup>4+</sup> ion surrounded tetrahedrally by four O<sup>2-</sup> ions (Figure 1)<sup>11</sup>. Each of these O ions has a negative charge, and so can connect to either another O<sup>-</sup> ion and thereby add to the network (denoted as a bridging oxygen (BO or O<sup>0</sup>)) or to a cation, thereby breaking the chain (denoted as a non-bridging oxygen (NBO or O<sup>-</sup>)). Oxygen ions that are not associated with Si ions are referred to as free oxygen (denoted O<sup>2-</sup>)<sup>11</sup>.

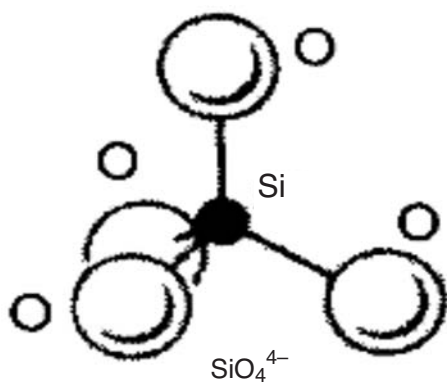


Figure 1—Silicate structure showing four O<sup>-</sup> in tetrahedral positions surrounding a Si<sup>4+</sup> ion

The structure of a slag can thus be represented by the mole fractions ( $X$ ) of O<sup>0</sup>, O<sup>-</sup> and O<sup>2-</sup> present. Consequently, it is customary to divide various constituents into either network formers (e.g. SiO<sub>2</sub>) or network breakers (CaO, Na<sub>2</sub>O, etc.). However, when Al<sub>2</sub>O<sub>3</sub> is added to a silicate slag, the Al<sup>3+</sup> ion can be absorbed into the Si<sup>4+</sup> chain but requires charge-balancing cations (e.g. Na<sup>+</sup> or 0.5Ca<sup>2+</sup>) to create a (NaAl)<sup>4+</sup> ion which must be located near the Al<sup>3+</sup> as shown in Figure 2. Cations on charge-balancing duties cannot act as network-breakers.

### Parameters used to represent structure

Several parameters have been used to represent the structure of the slag. The earliest models used the basicity (%CaO/%SiO<sub>2</sub>) or basicity indices where different weights were given to different basic oxides (e.g. CaO, MgO, or FeO). The most widely used parameter is the ratio of NBO to tetragonal ions (NBO/T), which is calculated using Equation [1]. NBO/T is a measure of the depolymerization of the slag.

$$\text{NBO/T} = \frac{2(X_{MO} + X_{M_2O} + 3fX_{M_2O_3} - X_{Al_2O_3} - (1-f)X_{M_2O_3})}{(X_{SiO_2} + 2X_{Al_2O_3} + 2(1-f)X_{M_2O_3})} \quad [1]$$

where  $X$  = mole fraction,  $f$  = fraction of  $M_2O_3$  acting as a network breaker  $MO=CaO, FeO$  etc.  $M_2O=Na_2O$  etc. and  $M_2O_3=Fe_2O_3, Cr_2O_3$  etc.

Some workers prefer using the parameter  $Q$  (defined in Equation [2]) since this provides a measure of the polymerization of the slag that is easier to visualize;  $Q$  will be used here. Table I provides some examples of the physical reality of various  $Q$  and (NBO/T) values.

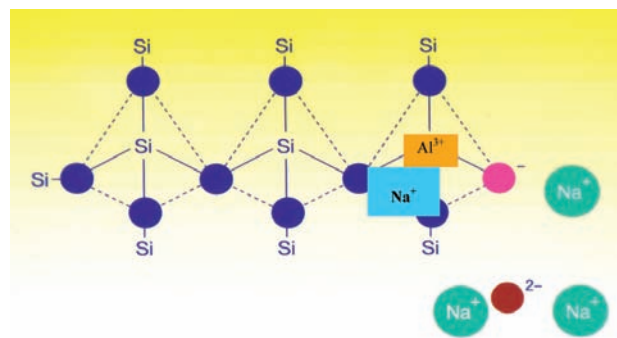


Figure 2—Formation of a silicate network showing (a) bridging oxygens and (b) charge-balancing by a Na<sup>+</sup> (denoted as a rectangle) when Al<sup>3+</sup> cations are incorporated into the network (denoted as a rectangle)

Table I  
NBO/T and Q for various CaO-SiO<sub>2</sub> slag compositions

Unit	Equivalent	NBO/T	Q	Examples
SiO <sub>4</sub> <sup>4-</sup> (monomer)	2CaO.SiO <sub>2</sub>	4	0	BOS slag ; Q=ca. 0
Si <sub>2</sub> O <sub>7</sub> <sup>6-</sup> (polyhedra)	3CaO.2SiO <sub>2</sub>	3	1	Mould flux; billets; Q= 1
Si <sub>2</sub> O <sub>6</sub> <sup>4-</sup> (chain)	CaO.SiO <sub>2</sub>	2	2	BF slag Q>2 Mould fluxes; Q= 2-2.5
Si <sub>2</sub> O <sub>5</sub> <sup>2-</sup> (sheet)	CaO. 2SiO <sub>2</sub>	1	3	Glasses, Coal slags
SiO <sub>2</sub> (3-dim)	SiO <sub>2</sub>	0	4	Glasses

## Estimating the physical properties of slags

$$Q=4-NBO/T \quad [2]$$

Other models<sup>10</sup> calculate the mole fractions of  $O^\circ$ ,  $O^-$ , and  $O^{2-}$  (which are usually calculated using the Gaye modification<sup>12</sup> of the Kapoor-Frohberg cell model<sup>13</sup>) and relate these to the property values.

Structural data for slags can be determined using Raman spectroscopy; in these cases the structural parameters can be expressed as the mole fractions of  $Q_1$  (equivalent to  $2CaO.SiO_2$  or  $O^{2-}$  units),  $Q_2$  ( $3CaO. 2SiO_2$  units),  $Q_3$  ( $CaO.SiO_2$  units), and  $Q_4$  ( $SiO_2$  or  $O^0$  units).

One difficulty when using both  $(NBO/T)$  and  $Q$  is that they do not differentiate between the effects of the different cations on the structure or property (e.g. CaO, MgO, and  $Na_2O$ ). For this reason, the optical basicity ( $\Lambda$ ) has been used to represent the structure as it does differentiate between cations but this parameter ( $\Lambda_{corr}$ ) is usually corrected for the cations used in charge-balancing duties<sup>14</sup>.

Du and Seetharaman<sup>15,16</sup> took a different approach and represented the activation energy for viscous flow as a function of the excess free energy ( $\Delta G^{xs}$ ) of the molten slag.

### Effect of different cations on properties

Property values are affected by the nature of the cation as can be seen from Table II. The cations affect the various properties in different ways:

- (i) Divalent ions (e.g.  $Ca^{2+}$ ) will break two different chains and the resulting ionic bonds hold these two chains together ( $O^-Ca^{2+}O^-$ ), whereas monovalent ions ( $O^-Na^+$ ) will break only one chain; consequently, for the viscosities of slags with equivalent compositions,  $\eta_{CaO} > \eta_{Na_2O}$ .
- (ii) For equivalent slag compositions (identical  $Q$ ) there are twice as many  $Na^+$  ions as  $Ca^{2+}$  ions; since the electrical conductivity is dependent upon the number of ions available, it follows that the electrical conductivity of  $K_{Na_2O} > K_{CaO}$ .
- (iii) The electrical conductivity is also dependent upon the mobility of the cations; thus it would be expected that the conductivity would be greater for smaller cations; this is valid for Li, Na, and K ions, but the reverse trend can be seen with Ba, Ca, and Mg. This is probably due to the effects of increased polarization with decreasing ionic radius that could also affect the cationic mobility.

Inspection of Table II indicates that, although property values are affected by different cations, the effect differs according to the property.

### Effect of temperature on physical properties

Increasing temperature tends to loosen the network structure. Thus properties such as viscosity and thermal conductivity tend to decrease with increasing temperature<sup>3</sup>. For other properties where the network offers a resistance to movement (e.g. electrical conductivity and thermal expansion), property values tend to increase with increasing temperature.

When looking at the effect of temperature on solid slags it is necessary to divide slags into (i) glassy slags and (ii) crystalline slags. It is customary to express structure-related properties (e.g. viscosity, electrical conductivity) by either the Arrhenius or Weymann equations shown in Equations [3] and [4] respectively, where  $A$  and  $B$  are constants and ( $B = E/R$ ) where  $E$  = activation energy for viscous flow and  $R$  = gas constant.

$$\eta(dPas) = A_A \exp(B_A/T) \quad [3]$$

$$\eta(dPas) = A_W T \exp(B_W/T) \quad [4]$$

$$\eta(dPas) = A_V \exp(B_V/(T-T_0)) \quad [5]$$

When heating a glassy slag from room temperature, there is an abrupt change in property (e.g.  $C_p$ ,  $\alpha$ ) at the glass transition temperature ( $T_g$ ) where the slag transforms into a supercooled liquid (*scl*). This transition at  $T_g$  is accompanied by a step-like increase in  $C_p$  and a 3-fold increase in  $\alpha$  above  $T_g$ . The viscosity of the *scl* decreases smoothly with increasing temperature above  $T_g$  and is usually expressed in the form of the Vogel-Fulcher relation (Equation [5]) with the viscosity value at  $T_g$ ,  $\eta_{T_g}(dPas) = 10^{13.4}$  (Figure 3a). Thus for supercooled liquids there are no abrupt changes in property at  $T_{liq}$  (e.g. no enthalpy of fusion). In contrast, when a liquid slag is cooled to the point where crystals are precipitated (known as the break temperature,  $T_{br}$ ) there is a sudden increase in viscosity (Figure 3b).

Heating a crystalline slag results in no abrupt changes in property at  $T_g$ , and both  $C_p$  and  $\alpha$  values tend to be lower than those of glassy slags for the region where  $T_g < T < T_{liq}$ . However, for crystalline slags, there is an abrupt change in both enthalpy ( $\Delta H_{fus}$ ) and volume ( $\Delta V_{fus}$ ) when the crystalline solid transforms to liquid in the fusion region. Thus it is necessary to differentiate between glassy and crystalline

Property	Structure dependence	Cation dependence	[Ref] Comments T dependence
$T_{liq}$		Mg>Ca>Sr>Ba>Li>Ca>Sr>Ba: $T_{liq} \uparrow$ as $(Z/r^2) \uparrow$	For same $X_{SiO_2}$
$\alpha, \beta$	$\alpha, \beta \uparrow$ as $Q \downarrow$	K>Na>Li>Ba>Ca>Mg; $\alpha \uparrow$ -as $(Z/r^2) \downarrow$	[3]
$k$	$k \uparrow$ as $Q \uparrow$	Li seems to $\uparrow k$ at 298& $T_g$	[3]
$\kappa$	$\kappa \uparrow$ as $Q \downarrow$ :	Li>Na>K>Ba>Ca>Mg; $\kappa_i > \kappa_{ii}$	[17]
$\eta$	$\eta \uparrow$ as $Q \uparrow$	$\eta_{Mg} > \eta_{Ca} > \eta_{Sr} > \eta_{Ba} > \eta_{Fe}$ : $-\eta \downarrow$ as $(Z/r^2) \downarrow$ $\eta_{Mg} > \eta_{Ba} > \eta_{Sr} > \eta_{Ca} > \eta_{Fe}$ :	[18] [19]

## Estimating the physical properties of slags

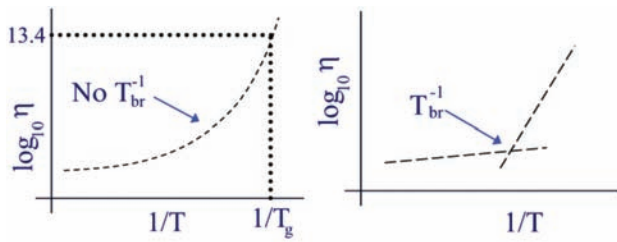


Figure 3—Plots of  $\log_{10}$  viscosity as functions for reciprocal temperature ( $K^{-1}$ ) for (a) glassy slag ( $Q>2.5$ ) and (b) for a less-glassy slag ( $Q=2$ )

slags when estimating property values in the solid state; as a rough rule of thumb, glassy slags occur when  $Q>2.5$  and crystalline slags when  $Q<2$ .

### Modelling thermo-physical properties of slags

The fundamentals underlying the various methods used to calculate individual properties in the program are described below. All temperatures in this paper refer to the thermodynamic temperature,  $K$ .

#### Liquidus temperature ( $T_{liq}$ )

It is essential to have a value for the liquidus temperature when modelling the thermo-physical properties of both solid and liquid slags. In the commercial thermodynamic models  $T_{liq}$  can be calculated for the temperature where the activity of the liquid is unity. This facility is not available for the present software and a value should be provided by the user. If the user does not provide a  $T_{liq}$  value, the model will insert a default value (Equation [6]). This was obtained by carrying out regression analysis on 124  $T_{liq}$  values taken from several sources<sup>20,21</sup>. This approach provides general trends for the effect of individual oxides on  $T_{liq}$ . However, the liquidus surface contains 'peaks and valleys' that frequently occur at compositions corresponding to compound formation, e.g. '2CaO.SiO<sub>2</sub>'. The database contains a number of  $T_{liq}$  values corresponding to such compounds. The mean uncertainty of the estimated  $T_{liq}$  value is  $\pm 130K$ . This is due mainly to large deviations ( $\pm 500K$ ) that can occur for compound 'peaks and valleys' which constitute about a quarter of the database; for the remainder of the database, the uncertainty is  $\pm 100K$ . For these reasons, users are recommended to provide a value if they have one.

$$T_{liq}(K) = 958 + 656.9X_{SiO_2} + 1040.7X_{CaO} + 1343.2X_{Al_2O_3} + 1090.5X_{MgO} + 137X_{Na_2O} - 668X_{K_2O} + 408.7X_{Li_2O} + 522X_{FeO} + 760.9X_{MnO} + 1022X_{CrO} + 794X_{Fe_2O_3} + 2198X_{Cr_2O_3} - 532X_{CaF_2} + 844X_{TiO_2} - 12.6X_{B_2O_3} + 1207X_{BaO} + 1768X_{SrO} + 2234X_{ZrO_2} \quad [6]$$

#### Glass transition temperature ( $T_g$ )

It is also essential to have a value of  $T_g$  for the estimation of the thermo-physical properties of solid, glassy materials. The following equation was derived by regression analysis of experimental data for  $T_g$  and chemical compositions of the slags.

$$T_g(K) = 1028 - 26X_{SiO_2} + 189.5X_{CaO} - 95.6X_{Al_2O_3} - 996X_{Na_2O} - 850X_{Li_2O} - 600X_{K_2O} - 59760X_{MgO} + 7034X_{CaF_2} - [7] \\ 6366X_{MnO} + 3608X_{FeO}$$

It should be noted that the constants associated with MgO, MnO, and FeO are 'unrealistic' since they are based on values for slags with ca. 1% of these oxides, which leads to unrealistic estimates of  $T_g$  when applied to slags with much higher concentrations of these oxides.

#### Heat capacity ( $C_p$ ) and enthalpy ( $H_T - H_{298}$ )

##### Crystalline slags

The heat capacities of slags are little affected by the structure of the slag; thus it is possible to obtain reasonable estimates of  $C_p$  from partial molar  $C_p$  values for individual components (Equation [8] where 1, 2 = CaO, SiO<sub>2</sub>, etc.).

$$C_p = \sum (X_1 C_{p1}) + (X_2 C_{p2}) + (X_3 C_{p3}) + (X_4 C_{p4}) \quad [8]$$

It is customary to express the temperature dependence of  $C_p$  of crystalline slags in the form:

$$C_p = a + bT - c/T^2 \quad [9]$$

Thus it is possible to derive individual values of the parameters,  $a$ ,  $b$ , and  $c$  by:<sup>19</sup>

$$a = \sum (X_1 a_1) + (X_2 a_2) + (X_3 a_3) + (X_4 a_4) \quad [10]$$

The enthalpy ( $H_T - H_{298}$ ) is given by

$$(H_T - H_{298}) = 298 \int C_p dT = a(T - 298) + 0.5bT^2 - 0.5b(298)^2 + (c/T) - (c/298) \quad [11]$$

Consequently, ( $H_T - H_{298}$ ) for the crystalline state can be calculated from the  $a$ ,  $b$ , and  $c$  values.

It takes energy for a crystalline solid to transform into a liquid slag, and this energy (enthalpy of fusion,  $\Delta H^{fus}$ ) can be calculated from the entropy of fusion ( $\Delta S^{fus}$ ) that represents the structural changes accompanying this transition. The  $\Delta H^{fus}$  can be calculated in the following way<sup>22</sup>:

$$\Delta S^{fus} = \sum (X_1 \Delta S^{fus}_1) + (X_2 \Delta S^{fus}_2) + [12] \\ (X_3 \Delta S^{fus}_3) + (X_4 \Delta S^{fus}_4) + \dots \\ \Delta H^{fus} = T_{liq} \Delta S^{fus} \quad [13]$$

##### Glassy slags

The  $C_p$  values for glassy slags are very similar to those of crystalline slags in the range (298K to  $T_g$ ), but glassy slags show a stepwise increase of ca. 0.2 kJ  $K^{-1}kg^{-1}$  at  $T_g$  ( $C_p T_g$  usually occurs around 1100 J  $K^{-1}kg^{-1}$  (=1.1 kJ  $K^{-1}kg^{-1}$ ). The enthalpy ( $H_T - H_{298}$ ) value at  $T_{liq}$  (=  $T^m$ ) for the liquid phase must be identical for both glassy and crystalline phases of the same composition. Thus we can calculate  $C_p$  and ( $H_T - H_{T_g}$ ) values by Equation [14] for the ( $T_g - T_{liq}$ ) range by assuming that  $C_p = a' + b'T$  in this range.

$$b' = 2\{(\Delta/(T^m - T_g)) - a'\} / (T^m + T_g) \quad [14]$$

where  $\Delta = (H_{T^m} - H_{298})_{crys} - (H_{T_g} - H_{298})_{glass}$  and  $a' = C_p^{scl} T_g$ . There is no enthalpy of fusion term at  $T_{liq}$  for the super-cooled liquid.

##### Liquid slags

Values for the liquid can be calculated from Equation [8] using the values  $C_p(l)$  for the various slag constituents (e.g. CaO, SiO<sub>2</sub>, etc.)<sup>22</sup>

## Estimating the physical properties of slags

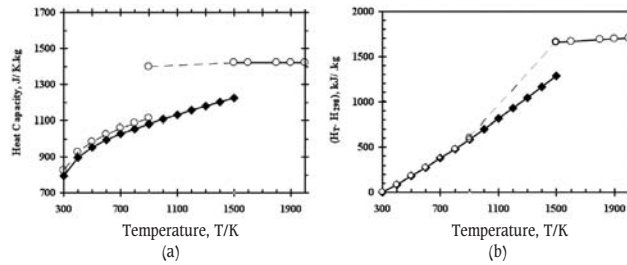


Figure 4—Schematic diagrams showing (a)  $C_p$  and (b) enthalpy ( $H_r - H_{298}$ ) of glassy and crystalline slags as functions of temperature; solid line,  $\diamond$ = crystalline phase; - - ,  $\circ$ = liquid, supercooled liquid and glass phases; vertical dotted lines represent  $T_g$  and  $T_{liq}$

### Density ( $\rho$ ) and Thermal expansion ( $\alpha$ , $\beta$ )

#### Liquid slags

The densities of most of the components of the slag tend to be similar, so Keene<sup>23</sup> proposed a simple relation for calculating the densities of molten steelmaking slags at 1673K with an uncertainty of ca.  $\pm 5\%$ .

$$\rho_{1673}(\text{kgm}^{-3}) = 2490 + 12 (\%FeO + \%Fe_2O_3 + \%MnO + \%NiO) \quad [15]$$

The densities of molten slags ( $\rho$ ) can be modelled<sup>19</sup> using the partial molar volumes ( $V$ , Equations [16] and [17], where  $M$ = molecular weight) of the various slag constituents. The effect of the  $SiO_2$  and  $Al_2O_3$  on the molar volume (i.e. structure) of the slag can be represented by simple relations (Equations [18] and [19] respectively) derived from an analysis of density measurements<sup>22</sup>. The densities are calculated for a reference temperature of 1773K and then adjusted to other temperatures by applying a temperature coefficient of  $-0.01\% \text{ K}^{-1}$ . The calculated densities usually lie within  $\pm 2\%$  of measured values.

$$V = \Sigma (X_1 V_1) + (X_2 V_2) + (X_3 V_3) + (X_4 V_4) + \dots \quad [16]$$

$$\rho = M/V \quad [17]$$

$$V_{SiO_2} = (19.55 + 7.97X_{SiO_2}) \quad [18]$$

$$V_{Al_2O_3} = (28.3 + 32X_{Al_2O_3} - 31.45X_{Al_2O_3}^2) \quad [19]$$

#### Solid slags

Thermal expansion coefficients ( $\alpha$ ) for crystalline and glassy slags are very similar for temperatures in the range (298K to  $T_g$ ). However, for glassy slags, the transition into a supercooled liquid ( $scl$ ) is accompanied by a three-fold increase in  $\alpha$ , whereas, in contrast, for crystalline slags,  $\alpha$  maintains its gradual increase with increasing temperature. Consequently, for any specific temperature in the range ( $T_g$  to  $T_{liq}$ ),  $V_T^{scl} > V_T^{crys}$ . However, at  $T_{liq}$ , there is a sudden increase in volume ( $\Delta V^{fus}$ ) as the crystalline solid transforms into a liquid; in contrast, there is no volume change associated with the transition of a  $scl$  into a liquid (i.e.  $\Delta V^{fus}=0$ ). Thus the enhanced volume change associated with  $\alpha^{scl}$  in the ( $T_g$  to  $T_{liq}$ ) range is offset by  $\Delta V^{fus}$ .

#### Crystalline slags

Slags with crystalline phases have a higher density than glassy, amorphous slags, and will show a marked change in

density at  $T_{liq}$  ( $\Delta\rho^{fus}$ ). The slag densities are estimated at 298 K by using a very similar method to that adopted for the liquid phase. The values at  $T > 298 \text{ K}$  were calculated by using an average linear thermal expansion coefficient ( $\alpha$ ) of  $9 \times 10^{-6} \text{ K}^{-1}$ .

#### Glassy slags

Molar volumes ( $V_T$ ) are calculated in an identical manner to that for crystalline phases up to  $T_g$ . For temperatures above  $T_g$ , the molar volume of  $scl$  ( $V_T$ ) is calculated using Equation [20] and the liquid molar volume at  $T_{liq}$  ( $V^m$ ) and the molar volume of the  $scl$  at  $T_g$  ( $V_{T_g}$ ):

$$V_T = V_{T_g} + (T - T_g) \{ (V^m - V_{T_g}) / (T_{liq} - T_g) \} \quad [20]$$

#### Viscosity ( $\eta$ )

Viscosity is a measure of the resistance encountered when moving one set of atoms over a lower layer of atoms. Thus, as the network structure becomes more polymerized (i.e.  $Q$  increases) the resistance to viscous flow will increase and thus the viscosity ( $\eta$ ) will increase. Since increased temperature loosens up the structure, the viscosity will decrease with increasing temperature. The viscosity has been used as a measure of the slag's structure<sup>5</sup>.

The Riboud<sup>24</sup>, Urbain<sup>25</sup>, and Iida<sup>26</sup> models have been implemented in the software.

#### Riboud model<sup>24</sup>

This model is simple and is applicable to a wide range of slags. The model divides the slag constituents into five different categories (see below). Additional slag constituents are covered in the software and these have been allocated to the various groups and are denoted by  $\{ \}$ . The model applies to the following ranges:  $SiO_2$  (28–48%),  $CaO$  (13–52%),  $Al_2O_3$  (0–17%),  $CaF_2$  (0–21%),  $Na_2O$  (0–27%).

$$X_{SiO_2}' = X_{SiO_2} + X_{P_2O_5} + X_{TiO_2} + X_{ZrO_2} \quad [21]$$

$$X_{CaO}' = X_{CaO} + X_{MgO} + X_{FeO} + X_{Fe_2O_2} + \{ X_{MnO} + X_{NiO} + X_{CrO} + X_{ZnO} + X_{Cr_2O_3} \} \quad [22]$$

$$X_{Al_2O_3}' = X_{Al_2O_3} + \{ X_{B_2O_3} \} \quad [23]$$

$$X_{CaF_2}$$

$$X_{Na_2O}' = X_{Na_2O} + X_{K_2O} + \{ X_{Li_2O} \} \quad [24]$$

The temperature dependence is expressed via the Weymann equation  $\{ \eta(dPas) = A_w T \exp(B_w/T) \}$  and the viscosity is calculated from this relation where  $A_w$  and  $B_w$  are calculated using Equations [25] and [26].

$$A = \exp(-19.81 + 1.73X_{CaO}' + 5.82X_{CaF_2} + 7.02X_{Na_2O}' - 35.76X_{Al_2O_3}) \quad [25]$$

$$B = 31140 - 23896X_{CaO}' - 46356X_{CaF_2} - 39159X_{Na_2O}' + 68833X_{Al_2O_3}' \quad [26]$$

#### Urbain model<sup>25</sup>

This model divides the various slag constituents into the following groups:

$$\text{Glass formers } X_G = X_{SiO_2} \quad [27]$$

Network modifiers:

$$X_M = X_{CaO} + X_{MgO} + X_{CaF_2} + X_{FeO} + X_{MnO} + X_{CrO} + X_{NiO} + X_{Na_2O}' + X_{K_2O} + X_{Li_2O} + 2X_{TiO_2} + X_{ZrO_2} \quad [28]$$

## Estimating the physical properties of slags

$$\text{Amphoterics: } X_A = X_{Al_2O_3} + X_{B_2O_3} + X_{Fe_2O_3} + X_{Cr_2O_3} \quad [29]$$

Here it has been assumed that  $Fe_2O_3$  and  $Cr_2O_3$  behave both as network breakers and as amphoteric, where  $f$  is the fraction ( $f$ ) behaving as network modifiers and a value  $f=0.6$  is assumed.

The Urbain model works predominantly on a basis of  $M_xO$  so this creates extra ions and it is necessary to normalize  $X_G$ ,  $X_M$ , and  $X_A$  by dividing by the term  $(1 + 0.5X_{FeO_{1.5}} + X_{TiO_2} + X_{ZrO_2} + X_{CaF_2})$  to give  $X_G^*$ ,  $X_M^*$  and  $X_A^*$ .

The model assumes the Weymann relation

$$\eta(dPas) = A_W T \exp(B_W/T) \quad [30]$$

Urbain<sup>25</sup> found that  $A$  and  $B$  were linked through the equation

$$-\ln A_W = 0.29B_W + 11.57 \quad [31]$$

The  $B_W$  value must be calculated via the equations

$$\alpha^* = X_M / (X_M + X_A) \quad [32]$$

$$B_i = a_i + b_i \alpha + c_i \alpha^2 \quad [33]$$

where subscript  $i$  can be 0, 1, 2, or 3 and  $a$ ,  $b$ , and  $c$  are given constants for each case e.g. 0, 1, 2, 3.

$$B = B_0 + B_1 X_{SiO_2} + B_2 X_{SiO_2}^2 + B_3 X_{SiO_2}^3 \quad [34]$$

Different values for  $a$ ,  $b$ , and  $c$  are given for 0,1,2,3 to calculate  $B$  values for the  $CaO-Al_2O_3-SiO_2$ ,  $MgO-Al_2O_3-SiO_2$ , and  $MnO-Al_2O_3-SiO_2$  systems. In this study, we have modified  $X_{MnO}$  to represent  $X_{MnO} + X_{FeO} + X_{NiO} + X_{CrO} + 0.6(X_{Fe_2O_3} + X_{Cr_2O_3})$ . The global  $B$  ( $B_{global}$ ) is given by

$$B_{global} = (X_{MnO} B_{MnO} + B_{CaO} X_{CaO} + B_{MgO} X_{MgO}) / (X_{MnO} + X_{CaO} + X_{MgO}) \quad [35]$$

The values calculated with this software are in good agreement with the values cited by Urbain<sup>24</sup> but the model does not have  $B_i$  values covering monovalent oxides (e.g.  $Na_2O$ ).

### Iida model<sup>26</sup>

The model<sup>26</sup> makes use of the basicity index ( $B_i$ ) to represent structure:

$$\eta(Pas) = A \eta_0 \exp(E/B_i) \quad [36]$$

where  $A$  = pre-exponential term,  $E$  = activation energy;  $\eta_0$  = hypothetical viscosity for each slag constituent ( $i$ ); the parameters  $A$ ,  $E$ , and  $\eta_0$  are all given as functions of temperature.

$$A = 1.029 - 2.078 \times 10^{-3}T + 1.05 \times 10^{-6}T^2 \quad [37]$$

$$E = 28.46 - 2.884 \times 10^{-2}T + 4.0 \times 10^{-6}T^2 \quad [38]$$

$$\eta_0 = \sum \eta_0 X_{SiO_2} + \eta_0 X_{CaO} + \eta_0 X_{Al_2O_3} + \eta_0 X_{MgO} + \dots \quad [39]$$

$$\eta_0 = 1.8 \times 10^{-7} \{ (M_i T_i^m)^{0.5} \exp(H_i / R^* T) \} / \{ V_m \}_i^{0.6667} \exp(H_i / RT) \quad [40]$$

where  $V_m$  = molar volume for each constituent, and  $H_i = 5.1 (T^m)_i$  and  $R^*$  = gas constant

The various constituents are divided into the following categories: (1) acidic ( $SiO_2$ ,  $ZrO_2$ ,  $TiO_2$ ) denoted by subscript A, (2) basic ( $CaO$ ,  $MgO$ ,  $Na_2O$ ,  $K_2O$ ,  $Li_2O$ ,  $FeO$ ,  $MnO$ ,  $CrO$ ,  $CaF_2$ , etc.) denoted by subscript B, and (3) amphoteric ( $Al_2O_3$ ,  $B_2O_3$ ,  $Fe_2O_3$ ,  $Cr_2O_3$ ). The basicity index  $B_i$  is calculated by

$$B_i = \sum (\alpha_i \%i)_B / \sum (\alpha_i \%i)_A \quad [41]$$

where  $\alpha_i$  = constant for each constituent expressing its relative basicity and  $\%i$  = mass %.

This was the original Iida model. Subsequently, the model was modified<sup>26</sup> to account for the amphoteric where their basicity changed according to the temperature. This was done through the modified basicity index ( $B_i^j$ ), particularly for  $Al_2O_3$ , which was done through back-calculation from experimental viscosity data (Equation [42]). It was concluded that  $Fe_2O_3$  and  $Cr_2O_3$  worked basically as basic oxides so they appear on the top line. The model gets exceedingly complicated because the modified  $\alpha$  (denoted  $\alpha^*$ ) for  $Al_2O_3$  was obtained from experimental viscosity data for certain systems, e.g.  $CaO + MgO + Al_2O_3 + SiO_2$ , and then expressed by Equation [42].

$$(B_i^j) = \{ \sum (\alpha_i \%i)_B + (\alpha_i \%i) Fe_2O_3 + (\alpha_i \%i)_{BCr_2O_3} \} / \{ \sum (\alpha_i \%i)_A + \sum (\alpha_i^* \%i) Al_2O_3 \} \quad [42]$$

$$\alpha_i^* = a B_i + b \%Al_2O_3 + c \quad [43]$$

It is difficult to apply the Iida model to systems where there is no experimental data since  $\alpha_i^*$  values are determined for each system/family and there is no general overall value for  $\alpha_i^*$ . For example, one can calculate  $\alpha_i^*$  from a, b, and c values for  $CaO + MgO + Al_2O_3 + SiO_2$  but other a, b, c values (leading to a different  $\alpha_i^* Al_2O_3$ ) are given for  $Li_2O + Al_2O_3 + SiO_2$ . The high accuracy claimed with this model comes from its calibration with experimental data for each family of slags.

### Thermal conductivity ( $k$ )

There are no extant models for estimating thermal conductivities but Mills<sup>3</sup> noted that the thermal conductivity of liquid silicate slags at  $T_{liq}$  ( $k^m$ ) increased linearly as  $(NBO/T)$  decreased (i.e.  $Q$  increased). Phonon conduction is considered to occur as lattice waves. Slags exhibit covalent bonding (in chains, etc.) and ionic bonding. Since  $k^m$  increases with increasing  $Q$ , it is obvious that thermal conduction is greater along the covalent chain than across the cationic bonds. Consequently, a relationship between thermal conductivity and viscosity might be expected, and recent work<sup>4,27</sup> has shown that such a link exists. Further evidence for this link between thermal conductivity and viscosity lies in the temperature dependence of the thermal conductivities of molten slags that can be satisfactorily represented by the Arrhenius relation, which is widely used for the temperature dependence of viscosity<sup>27,28</sup>.

Thermal conductivity ( $k_R$ ) measurements at temperatures on glassy and liquid slags contain a significant and unknown contribution from radiation conduction<sup>29</sup>. These  $k_R$  contributions are much smaller in transient hot wire (THW) measurements than for those obtained with the laser pulse (LP) method, because the emitting surface area in LP experiments is 10x that in THW studies. Therefore, only thermal conductivity data from THW studies were accepted here. Typical examples of the temperature dependence of glassy, crystalline, and liquid slags are shown in Figure 5. The maximum in  $k$  occurs at  $T_g$  and it is our contention that the thermal conductivity in the range ( $T_g$  to  $T_{liq}$ ) can be represented by a Vogel-Fulcher relation (see Equation. [5]), which is widely used for viscosities in this range.

## Estimating the physical properties of slags

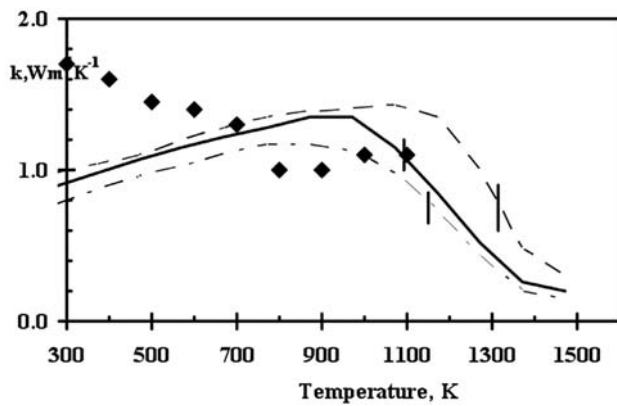


Figure 5—Thermal conductivity as a function of temperature for  $\text{Na}_2\text{O}.2\text{SiO}_2$  (dash-dot line),  $\text{Na}_2\text{O}.3\text{SiO}_2$  (solid line), and  $\text{Na}_2\text{O}.4\text{SiO}_2$  (dashed line)<sup>29</sup>,  $\blacklozenge$ =crystalline  $\text{CaO}.\text{SiO}_2$ <sup>30</sup>; vertical lines; solid= $T_{liq}$  and dotted= $T_g$ , it can be seen that  $k$  increases with increasing  $\text{SiO}_2$  content (i.e. increasing  $Q$ )

### Liquid slags

#### Method 1—relation with viscosity

This uses the relation of thermal conductivity ( $k$ ) of the liquid at  $T_{liq}$  ( $k^m$ ) with viscosity. Reported line source data for  $\ln k^m$ <sup>4,27,30-32</sup> were correlated with Riboud calculations of  $\ln \eta^m$ <sup>24</sup>. The data showed some scatter because of (i) uncertainties in the calculated  $\ln \eta^m$  values, (ii) experimental uncertainties associated with  $\ln k^m$ , and (iii) sensitivities of both  $\eta^m$  and  $k^m$  in the region around  $T_{liq}$  and the uncertainties in  $T_{liq}$  itself. The following relation was obtained.

$$\ln k^m = -2.178 + 0.282 \cdot \ln \eta^m \quad [44]$$

#### Method 2—relation to both $Q$ and $\ln \eta^m$

This method is similar to Method 1 in that it uses a relation between  $\ln \eta^m$  and  $\ln k^m$ . The data is shown in Figure 6, and has been expressed as an exponential relation.

$$\eta^m = 0.165 \exp(Q / 0.817) \quad [45]$$

Then  $\ln k^m$  can be calculated using the equation

$$\ln k^m = -1.8755 - 0.0893 (\ln \eta^m) + 0.0352 (\ln \eta^m)^2 \quad [46]$$

The values of  $k^m$  obtained are valid only for the range  $Q = 2$  to  $3.2$ . Care should be taken particularly for slags with  $Q > 3.2$  and for slags with high  $\text{Al}_2\text{O}_3$  contents (e.g. 45%  $\text{CaO}$  + 10%  $\text{SiO}_2$  + 45%  $\text{Al}_2\text{O}_3$  which would show a high  $Q$  value but, in actual fact, is largely made up of calcium aluminates and will show relatively low  $\eta^m$  and  $k^m$  values).

#### Method 3—relation with $Q$

The relation between  $\ln k^m$  and  $Q$  is shown in Figure 6b and it can be seen that it has similarities to the equation between  $\ln \eta^m$  and  $Q$  (Figure 6a, Equation [47]). There is significant dispersion in the scattered data for  $k^m$  but the upward trend with increasing  $Q$  is obvious. Unfortunately, the experimental values for  $k^m$  lie within the range  $Q = 2$  to  $3.2$ . The following relation was derived:

$$\ln k^m = -1.914 + 0.00037 \exp(Q/0.402) \quad [47]$$

This equation is valid only for the range  $Q = 2$  to  $3.2$ .

The temperature dependence would be expected to follow an Arrhenius-type relation because of the correlation between  $\eta$  and  $k$ .

$$\ln k_T(l) = A \exp(B/T) \quad [48]$$

There are insufficient data to determine  $B$  values as a function of  $Q$ , so an approximate relation for  $dk/dT$  was obtained but should be used with caution.

$$dk/dT = 0.0005 \exp(0.5551Q) \quad [49]$$

### Solid slags

#### Method 1

The experimental data for  $\ln k_{298}$  and  $\ln k_{T_g}$  show appreciable scatter when plotted vs  $Q$ , but they do show  $k$  increasing with increasing  $Q$ . The data were assumed to follow an exponential relation similar to that used for  $\ln \eta^m$  (Equation [47], Figure 6b). It was noted that the experimental data for solid  $\text{Li}_2\text{O}$ -containing slags were significantly higher than the curve values and so a correction for  $\text{Li}_2\text{O}$  was added to the exponential relation:

$$\ln k_{298} = -0.424 + 0.00002 \exp(Q / 0.299) + 3.2 X_{\text{Li}_2\text{O}} \quad [50]$$

$$\ln k_{T_g} = -0.435 + 0.00005 \exp(Q / 0.332) + 3.0 X_{\text{Li}_2\text{O}} \quad [51]$$

This equation should not be used out of range i.e.  $Q > 3.3$  or  $Q < 2$ .

Values can be calculated at other temperatures by linear interpolation between  $298 \text{ K}$  and  $T_g$ , and values have also been calculated in the same manner for  $T_g$  to  $T_{liq}$  (but this should in fact follow a Vogel-Fulcher relation, Equation [5], but there was not enough data to establish the necessary constants). This procedure should be accepted only for slags in the range  $Q = 2$  to  $3.3$ .

#### Method 2

A second method is also shown. It was found that for slags with  $Q$  around  $2.5$  the thermal diffusivity between  $298 \text{ K}$  and  $T_g$  tends to have a constant value  $a = 4 \times 10^{-7} \text{ m}^2\text{s}^{-1}$ . Values calculated from  $k = a \cdot C_p \cdot \rho$  using the calculated values of  $C_p$  and  $\rho$  are also shown. These values apply only when  $Q = 2$  to  $3$ .

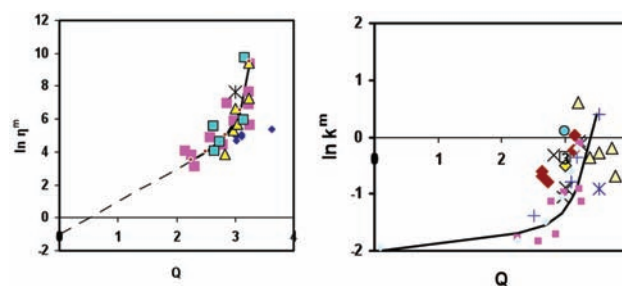


Figure 6—(a) Viscosity and (b) thermal conductivity at the liquidus temperature as function of the parameter  $Q$

## Estimating the physical properties of slags

### Crystalline slags

Nishioka *et al.*<sup>31</sup> report that  $k$  values for crystalline slags are between 1.5 and 2.5 times higher than that for the glassy slag and are independent of temperature (Figure 5). Thus it has been assumed that  $k_{crist} = 2k_{glass}$  and is independent of temperature from 298 to 1000K.

### Electrical conductivity ( $\kappa$ ) of liquid slags

The electrical conductivity involves the movement of cations under the influence of an applied field. In this case, the polymeric silicate network hinders the movement of the cations. Thus the factors affecting the electrical conductivity ( $\kappa$ ) are (i) the concentration, charge, and size of the cations and (ii) the polymeric network (as represented by  $Q$ ) which hinders the movement of cations. Smaller cations are more mobile, but the increased mobility of smaller cations is offset by the increased polarization in the M-O bond. For instance, for  $M_2O-SiO_2$  slags, the hierarchy is  $\kappa_{Li} > \kappa_{Na} > \kappa_K$  i.e. decreasing with increasing cation radius. However, the trend is reversed for the  $MO-SiO_2$  slags where  $\kappa_{Ba} > \kappa_{Sr} > \kappa_{Ca} > \kappa_{Mg}$ <sup>5,16</sup> i.e.  $\kappa$  decreases as  $(z/r^2)$ , possibly because of the higher charge ( $z$ ) in this slag series which would be expected to increase polarization. As increasing temperature gradually loosens up the structure, the hindrance to the movement of cations by the silicate network is reduced, and hence the conductivity increases with increasing temperature. It should also be noted that factors causing an increase in electrical conductivity would cause a decrease in thermal conductivity. The electrical conductivities of slags containing  $Li^+$ ,  $Na^+$ , and  $K^+$  are significantly higher than those containing  $Ca^{2+}$ ,  $Mg^{2+}$ , etc., because, for an equivalent slag structure ( $Q$ ),  $n_{Na^+} = n_{Ca^{2+}}$  where  $n$  = number of cations present.

The electrical conductivities have been estimated using recent papers by Zhang and Chou<sup>5, 36</sup>, both of which involve using the relation between conductivity and viscosity.

#### Method 1

Chou and Zhang<sup>35, 5</sup> proposed a relationship for slags containing  $CaO$ ,  $MgO$ ,  $Al_2O_3$ , and  $SiO_2$ .

$$\ln \kappa = (-0.08 - \ln \eta) / 1.18 \quad [52]$$

Zhang calculated values of  $\ln k$  using this equation and parameters to calculate the viscosity. These parameters are not generally available for all slag systems, so  $\ln \eta$  values were calculated here using the Riboud, Iida, and Urbain models.

#### Method 2

Zhang *et al.*<sup>5,36</sup> reported that the following equations apply for  $M_2O-SiO_2$  (where  $M_2O = Na_2O$  etc.) and  $MO-SiO_2$  (e.g.  $CaO$ ) systems.

$$M_2O-SiO_2: \quad \ln \kappa = (0.02 - \ln \eta) / 2.87 \quad [53]$$

$$MO-SiO_2 \quad \ln \kappa = (0.15 - \ln \eta) / 1.1 \quad [54]$$

The model assumes (i) that cations on charge balancing duties are not available for electrical conduction and (ii) the charge balancing is directly related to the concentrations of the various cations present (i.e. a statistical distribution). The differences between Equations [53] and [54] were attributed to the fact that there are twice as many  $Na^+$  ions as  $Ca^{2+}$  for equivalent compositions. Here the model calculates the ratio

( $r^*$ ) of  $M^+$  ions present in the slag (Equation [55]) and then calculates the conductivity using Equation [56] (which was derived from the product of  $r^*$  multiplied by the differences between Equations [53] and [54]). It is recommended that this method be used when the slag contains  $M^+$  ions e.g.  $Na^+$ ,  $K^+$ , or  $Li^+$ .

$$r^* = 2 \sum X_{M^+} / \sum (2 X_{M^+} + X_{M^{2+}} + 0.667 X_{M^{3+}} + 0.5 X_{M^{4+}}) \quad [55]$$

$$\ln \kappa = 0.15 + r^* 3.87 - (\ln \eta / \{1.1 + 1.77 r^*\}) \quad [56]$$

### Surface tension ( $\gamma$ )

#### Method 1

Surface tension is not a bulk property but is a surface property. The free surface of the molten slag contains higher concentrations of the constituents with lower surface tension. Values of surface tension and the trends in surface tension can be calculated using a partial molar approach (Equation [57]), and are shown in Figure 7<sup>37</sup>. The model divides slag components into two classes: (i) oxides with higher surface tension values where values of  $X_2 \gamma_2$  tend to be similar to that shown in Figure 7a and (ii) components with lower  $\gamma$  values (surfactants  $B_2O_3$ ,  $CaF_2$ ,  $Na_2O$ ,  $K_2O$ ,  $Fe_2O_3$ , and  $Cr_2O_3$ ) where values of  $X_2 \gamma_2$  tend to be similar to those shown in Figure 7a.

$$\gamma \text{ (mNm}^{-1}\text{)} = \sum X_1 \gamma_1 + X_2 \gamma_2 + X_3 \gamma_3 + \dots \quad [57]$$

These surface active components cause a rapid decrease in surface tension and, in these cases,  $X_2 \gamma_2$  and can be represented by two curves determined by a critical point N (corresponding to the minimum in Figure 7b) (i) for  $<N$  as a polynomial by  $X_2 \gamma_2 = a + bX + cX^2$  and (ii)  $>N$  by  $X_2 \gamma_2 = a' + b'X$  (which are shown by the dashed line in Figure 7b). The method has the advantage that it can easily be applied to multicomponent industrial slags, but uncertainties in the estimated values are ca.  $\pm 10\%$ . The biggest problem with this method lies in its inability to deal with two, or more, surface-active components simultaneously (e.g.  $CaF_2$  and  $B_2O_3$ ) and, for these conditions, Method 1 tends to exaggerate the decrease in  $\gamma$  in these cases (i.e.  $\gamma_{meas} > \gamma_{calc}$ ).

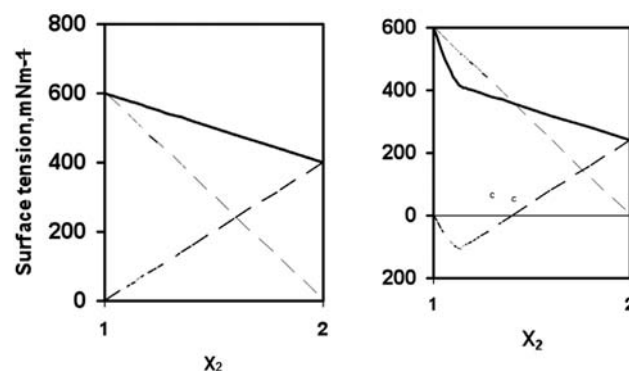


Figure 7—Schematic diagram showing compositional dependence ( $X$ ) of surface tension ( $\gamma$  = solid line) and  $X_1 \gamma_1$  and  $X_2 \gamma_2$  (= dashed lines) for a binary slag system containing (a) no surface active constituents and (b) one surface active constituent where 1 and 2 represent the slag components



## Estimating the physical properties of slags

### Method 2

Method 2 was devised to address this problem. It was assumed that (i) occupation of the surface occurs in the hierarchy (of lowest surface tension)  $B_2O_3 > K_2O > Na_2O > CaF_2 > Fe_2O_3 > Cr_2O_3$  and (ii) surface saturation occurs at  $N=0.12$ . The various surfactant contributions were calculated from the various oxides until the value  $N=0.12$  was attained. When  $N > 0.12$  all contributions from these surfactants were taken as positive contributions ( $=X_i\gamma_i$ ) i.e. they were not considered to be present in the surface layer and thus contributed normally to the bulk surface tension. The values calculated using Method 2 are preferred.

Most slags have negative temperature coefficients ( $d\gamma/dT$ )<sup>20</sup>. However, it is known that slags with high  $SiO_2$  contents exhibit positive ( $d\gamma/dT$ ) values<sup>38</sup>. This is related to the fact that  $SiO_2$  has a relatively low surface tension value. Ideally, ( $d\gamma/dT$ ) could be calculated on a partial molar basis but we do not have ( $d\gamma/dT$ ) data for all the slag constituents. Consequently, a constant value of ( $d\gamma/dT$ ) has been assumed. However, ( $d\gamma/dT$ ) values were calculated on a partial molar basis for those slag constituents where data were available (e.g. Equation [58]).

$$(d\gamma/dT) \text{ (mNm}^{-1}\text{K}^{-1}\text{)} = \sum X_1 (d\gamma_1/dT) + X_2 (d\gamma_2/dT) + X_3 (d\gamma_3/dT) + \dots \quad [58]$$

### Using the software

The intention behind this work is to provide a practical set of models that can be used by process engineers as working tools in everyday pyrometallurgical work. The software is available from <http://www.pyrometallurgy.co.za/KenMills/>, initially in the form of a spreadsheet, but other interactive calculation methods may be available in due course. The attractive feature of having the software available on a website is that the latest version can always be available to all users, and the burden of sending out software updates is relieved. Specific detailed instructions for the use of the software are available on the same website, so are not repeated here. The software requires the specification of the composition and liquidus temperature of the slag. If the glass transition temperature for glassy slags is known, this can also be specified; otherwise this will be estimated by the software.

### Acknowledgements

The authors would like to express their thanks to the following for their valuable comments during the preparation of this paper: Professor Seshadri Seetharaman (KTH, Stockholm), Professors M. Susa and M. Hiyashi (Tokyo Institute of Technology), Professor K. Morita and Dr Y. Kang (University Tokyo), and Professor K.C. Chou and Dr G.H. Zhang (University of Science and Technology Beijing).

### References

- MILLS, K.C. and FOX, A.B. The role of mould fluxes in continuous casting—so simple yet so complex. *ISIJ International*, vol. 43, 2003. pp. 1479–1486.
- JONES, R.T., REYNOLDS, Q.G., CURR, T.R., and SAGER, D. Some myths about DC arc furnaces. *Southern African Pyrometallurgy 2011*. Jones, R.T. and Den Hoed, P. (eds.). *Southern African Institute of Mining and Metallurgy*, Johannesburg, 6–9 March 2011. pp.15–32.
- MILLS, K.C. The influence of structure on the physico-chemical properties of slags. *ISIJ International*, vol. 33, 1993. pp. 148–156.
- HAYASHI, M., ISHII, H., SUSU, M., FUKUYAMA, H., and NAGATA, K. Effect of ionicity of nonbridging oxygen ions on thermal conductivity of molten alkali silicates. *Physics and Chemistry of Glasses - European Journal of Glass Science and Technology Part B*, vol. 42, no. 1, 2001. pp. 6–11.
- ZHANG, G.H. and CHOU, K.C. Simple method for estimating the electrical conductivity of oxide melts with optical basicity. *Metallurgical and Materials Transactions B*, vol. 41, no. 1, February 2010. pp. 131–136.
- NATIONAL PHYSICAL LABORATORY. MTDATA. [www.npl.co.uk/mtdata/](http://www.npl.co.uk/mtdata/)
- FactSage [www.factsage.com](http://www.factsage.com)
- THERMO-CALC SOFTWARE [www.thermocalc.com](http://www.thermocalc.com)
- TASKINEN, P., GISBY, J., PIHLASALO, J., and KOLHINENT, T. Validation of a new viscosity database with industrial smelting slags. *Proceedings, European Metallurgical Conference EMC2009*, Innsbruck, Austria, 28 June–1 July 2009. GDMB, Clausthal-Zellerfeld, Germany. vol. 3, pp. 915–930.
- LING ZHANG, SUN, S., and JAHANSHAH, S. Review and modeling of viscosity of silicate melts: Part I. Viscosity of binary and ternary silicates containing CaO, MgO, and MnO. Part II. Viscosity of melts containing iron oxide in the CaO-MgO-MnO-FeO-Fe<sub>2</sub>O<sub>3</sub>-SiO<sub>2</sub> system. *Metallurgical and Materials Transactions B*, vol.29, 1998. pp. 177–186 and 187–195.
- MYSEN, B.O. *Structure and Properties of Silicate Melts*. Elsevier, Amsterdam, 1988.
- GAYE, H and WELFRINGER, J. Modelling of the thermodynamic properties of complex metallurgical slags. *Proceedings of the 2nd International Symposium on Metallurgical Slags and Fluxes*. Fine, H.A. and Gaskell, D.R. (eds.). *The Metallurgical Society of AIME*, Warrendale, PA, 1984. pp. 357–373.
- KAPOOR, M.L. and FROHBERG, M.G. *Chemical Metallurgy of Iron and Steel*. *Iron and Steel Institute*, London, 1971. pp. 17–21.
- MILLS, K.C. and SRIDHAR, S. Viscosities of ironmaking and steelmaking slags. *Ironmaking & Steelmaking*, vol.26, no. 4, 1999. pp. 262–268.
- DU SICHEN, BYGDEN, J., and SEETHARAMAN, S. A model for estimation of viscosities of complex metallic and ionic melts. *Metallurgical and Materials Transactions B*, vol. 25, 1994. pp. 519–525.
- DU SICHEN, BYGDEN, J., and SEETHARAMAN, S. Estimation of the viscosities of binary metallic melts using Gibbs energies of mixing. *Metallurgical and Materials Transactions B*, vol. 25, 1994. pp. 589–595.
- MORINAGA, K., SUGINOHARA, T., and YANAGASE, T. The electrical conductivity of CaO-SiO<sub>2</sub>-Fe<sub>2</sub>O<sub>3</sub> and Na<sub>2</sub>O-SiO<sub>2</sub>-Fe<sub>2</sub>O<sub>3</sub> melts. *Journal of the Japan Institute of Metals*, vol. 39, 1975. pp. 1312–1317.

## Estimating the physical properties of slags

18. BOCKRIS, J. O'M., MACKENZIE, J.D., and KITCHENER, J.A. Viscous flow in silica and binary liquid silicates. *Transactions of the Faraday Society*, vol. 57, 1955. pp. 1734–1748.
19. URBAIN, G. *Revue Internationale des Hautes Temperatures et des Refractaires*, vol. 11, 1974. p. 133.
20. Slag Atlas. VDEh, Dusseldorf, 1995.
21. FORSBACKA, L. Experimental study and modelling of viscosity of chromium containing slags. PhD thesis, Helsinki University of Technology, Finland. 2007. (TKK-MT-196).
22. MILLS, K.C. and KEENE, B.J. Physical properties of BOS slags. *International Materials Reviews*, vol. 32, 1987. pp. 1–120.
23. KEENE, B.J. Ref 20 page 44.
24. RIBOUD, P.V., ROUX, Y., LUCAS, L.D., and GAYE, H. Improvements of continuous casting powders. Fachber. *Huttenpraxis Metallweitereverarb.*, vol. 19, 1981. pp. 859–869.
25. URBAIN, G. Viscosity estimation of slags. *Steel Research*, vol. 58, 1987. pp. 111–116.
26. IIDA, T. Proceedings of the Mills Symposium, London, 2002. Aune, R.E. and Sridhar, S. (eds.). *National Physical Laboratory*, Teddington, UK. see also CAMP-ISIJ 2002 15(4).
27. MILLS, K.C., YUAN, L., and LI, Z. Unpublished results. *Imperial College*, London, 2011.
28. KANG, Y. and MORITA, K. Thermal conductivity of the CaO–Al<sub>2</sub>O<sub>3</sub>–SiO<sub>2</sub> system. *ISIJ International*, vol. 46, 2006. pp. 420–426.
29. GARDON, R. *Proceedings of the 2nd International Thermal Conductivity Conference*, Ottawa, Canada, 1962. pp. 167.
30. NAGATA, K. *Proceedings Of the 2nd International Conference on Metallurgical Slags and Fluxes*, Lake Tahoe, NV, USA (1984) pp. 875.
31. NISHIOKA, K., MAEDA, T., and SHIMIZU, M. Application of square-wave pulse heat method to thermal properties measurement of CaO–SiO<sub>2</sub>–Al<sub>2</sub>O<sub>3</sub> system fluxes. *ISIJ International*. vol.46, 2006. pp. 427–433.
32. OZAWA, S., ENDO, R., and SUSU, M. Thermal conductivity measurements and prediction for R<sub>2</sub>O–CaO–SiO<sub>2</sub> (R=Li, Na, K) slags Tetsu-to-Hagane, vol. 93, no. 6, 2007. pp. 416–423.
33. OZAWA, S. and SUSU, M. Effect of Na<sub>2</sub>O additions on thermal conductivities of CaO–SiO<sub>2</sub> slags. *Ironmaking and Steelmaking*, vol. 32, no. 6, 2005. pp. 487–493.
34. SUSU, M., KUBOTA, S., HAYASHI, M., and MILLS, K.C. Thermal conductivity and structure of alkali silicate melts containing fluorides. *Ironmaking and Steelmaking*, vol. 28, no.5, 2001. pp. 390–395.
35. SUSU, M., WATANABE, M., OZAWA, S., and ENDO, R. Thermal conductivity of CaO–SiO<sub>2</sub>–Al<sub>2</sub>O<sub>3</sub> glassy slags: its dependence on molar ratios of Al<sub>2</sub>O<sub>3</sub>/CaO and SiO<sub>2</sub>/Al<sub>2</sub>O<sub>3</sub>. *Ironmaking and Steelmaking*, vol. 34, no. 2, 2007. pp. 124–130.

36. ZHANG, G.H., YAN, B.J., CHOU, K.C., and LI, F.S. Relation between viscosity and electrical conductivity of silicate melts. *Metallurgical and Materials Transactions B*, vol. 42, no.2, 2011. pp. 261–264.
37. MILLS, K.C. Estimation of physicochemical properties of coal slags. ACS Symposium Series 301, Mineral Matter and Ash in Coal. Vorres, KS (ed.). *American Chemical Society*, Washington DC, 1986. pp. 195–214.
38. MUKAI, K. and ISHIKAWA, T. *Nippon Kinzoku Gakkaishi*, vol. 45, no. 2, 1981. pp. 147.

### Symbols, abbreviations, units

$a$	= Thermal diffusivity (m <sup>2</sup> s <sup>-1</sup> )
$C_p$	= Heat capacity (JK <sup>-1</sup> /mol <sup>-1</sup> or JK <sup>-1</sup> /kg <sup>-1</sup> )
$E$	= Activation energy (kJ mol <sup>-1</sup> )
$f$	= Fraction of M <sup>3+</sup> ions acting as network breaker
(H <sub>T</sub> –H <sub>298</sub> )	= Enthalpy (Jmol <sup>-1</sup> or Jkg <sup>-1</sup> )
$\Delta H_{\text{fus}}$	= Enthalpy of fusion (Jmol <sup>-1</sup> or Jkg <sup>-1</sup> )
$k$	= Thermal conductivity (Wm <sup>-1</sup> K <sup>-1</sup> )
(l)	= Liquid phase
$M$	= Molecular weight (g mol <sup>-1</sup> )
$p$	= Partial pressure (atm, bar)
$Q$	= 4-(NBO/t)= measure of polymerization
$R$	= Gas Constant= 8.314 (J mol <sup>-1</sup> K <sup>-1</sup> )
$r$	= Cation radius (10 <sup>-10</sup> m)
(s)	= Solid phase
$scl$	= Supercooled liquid
$T$	= Temperature (K or °C)
$T_g$	= Glass transition temperature (K or °C)
$T_{liq}$	= Liquidus temperature (K or °C)
$V$	= Molar volume (m <sup>3</sup> mol <sup>-1</sup> )
$Z$	= Charge on cation (=2 for Fe <sup>2+</sup> )
$\alpha$	= Linear thermal expansion coefficient (K <sup>-1</sup> )
$\beta$	= Volume thermal expansion coefficient (K <sup>-1</sup> )
$\gamma$	= Surface tension (mNm <sup>-1</sup> )
$\gamma_{ms}$	= Slag/metal interfacial tension (mNm <sup>-1</sup> )
$\kappa$	= Electrical conductivity (Ω <sup>-1</sup> m <sup>-1</sup> )
$\Lambda$	= Optical basicity
$\eta$	= Viscosity (Pas or dPas)
$\theta$	= Contact angle (°)
$\rho$	= Density (kgm <sup>-3</sup> )
$BO$	= Bridging oxygen (O <sup>o</sup> )
$NBO$	= Non-bridging oxygen ((O <sup>-</sup> ))

### Subscripts

$br$	= Break (temperature)
$liq$	= Liquidus
$m(\text{subscript})$	= Metal
$s$	= Slag
$sol$	= Solidus

### Superscripts

$m(\text{superscript})$	= Value at $T_{liq}$ ◆
-------------------------	------------------------